

Polar Cap Disturbances: Mesosphere and Thermosphere – Ionosphere Response to Solar-Terrestrial Interactions

G. Sivjee¹, D. McEwen², and R. Walterscheid³

¹Embry-Riddle Aeronautical University

²University of Saskatchewan

³The Aerospace Corporation

Received: 7.12.2001 – Accepted: 16.5.2002

Abstract. The Polar Cap is the Upper-Atmosphere cum Magnetosphere region which is enclosed by the poleward boundary of the Auroral Oval and is threaded by open geomagnetic field lines. In this region, there is normally a steady precipitation (Polar “drizzle”) of low energy (~ 300 eV) electrons that excite optical emissions from the ionosphere. At times, enhanced ionization patches are formed near the Dayside Cusp regions that drift across the Polar Cap towards the Night Sector of the Auroral Oval. Discrete auroral arcs and auroras formed during Solar Magnetic Cloud (SMC) / Coronal Mass Ejection (CME) events are also observed in the Polar Cap. Spectrophotometric observations of all these Polar Cap phenomena provide a measure of the average energy as well as energy flux of the electrons precipitating in the Polar Cap region during these disturbances. Such measurements also point to modulations of the Polar Cap Mesosphere-Lower Thermosphere (MLT) air density and temperature by zonally symmetric tides whose Hough functions peak in the Polar region. MLT cooling during Stratospheric Warming events and their relation to Polar Vortex and associated Gravity wave activities are also observed at the Polar Cap sites.

ffects of Solar Magnetic Cloud (SMC) / Coronal Mass Ejection (CME) events (Sivjee and Shen, 1997) are observed in the Polar Cap region. An additional energy input, of solar origin, in the Arctic (and Antarctic) IT region comes in the form of enhanced Electro-Magnetic fields that lead to Joule heating (Thayer et al., 1998); the effects of the latter propagate to lower latitudes. The composition and the thermodynamics of the Polar Mesosphere and Lower Thermosphere (MLT) region are modulated by various quasi-periodic disturbances, including tides (Sivjee et al., 1994). A rich spectrum of the modulations of the high latitude MLT region is observed where specific Hough functions peak. Such tides have been shown to be zonally symmetric (Walterscheid and Sivjee, 2001). Very low frequency waves (with periods similar to those of Intraseasonal variations of the troposphere and stratosphere) are also observed in the Arctic and Antarctic Mesopause region (Sivjee and Walterscheid, 2001). The coupling among various Polar upper atmospheric regions is exemplified by Stratospheric Warming events that lead to Mesopause cooling (Walterscheid et al., 2001). Such events are related to the Polar Vortex and the associated Gravity Wave phenomena (Duck et al., 1998).

1 Introduction

The geomagnetic field configuration leads to the precipitation of electrons and protons (of solar origin) in the Polar region, giving rise to changes in composition and thermodynamics of the high latitude Thermosphere and Ionosphere (IT). The effects of these disturbances in the Polar region eventually propagate to lower latitudes. Even in the open geomagnetic field region of the Polar Caps, there is frequently a Polar “drizzle” of low energy (~ 300 eV) electrons (McEwen and Harrington, 1991), which excite very low level (subvisual) Polar Cap Ionosphere glow. At times, Polar Auroral Arcs (Zhang et al., 1998) and enhanced ionization patches (Weber et al., 1986) occur in the Polar Cap region. The ef-

2 Measurements

We operate high through-put electro-optical remote-sensing facilities, at several Polar stations, at all times when the local solar depression angle exceeds six degrees. The optical systems consist of Infrared Michelson Interferometers (MI) (Sivjee et al., 1994) and CCD Spectrographs (CCDS) (Sivjee and Shen, 1997). Measurements of absolute brightness and spectral distributions of airglow and auroral emissions with these facilities provide information about the abundance and thermodynamics of the Upper Atmospheric species.

Correspondence to: G. Sivjee

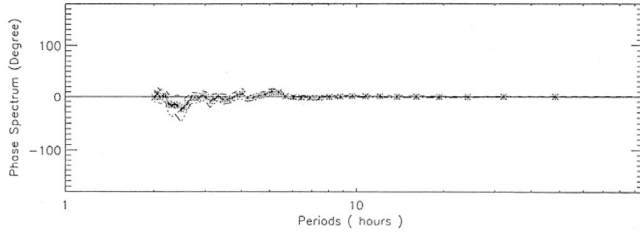


Fig. 1. Phase angle periodogram

3 Results

3.1 Arctic MLT Air Density and Temperature Fluctuations

Upper atmospheric Tidal and Planetary oscillations modulate the MLT air density and temperature leading to fluctuations in airglow brightness and rotational population distribution of MLT molecules, such as OH and O_2 , which radiate airglow band emissions. For a given tidal frequency ($f = 1/T = \omega/2\pi$) and zonal wave number (s), the tidal quantities, that generate airglow brightness and temperature changes, have a latitudinal dependence given by a linear combination of Hough functions (Walterscheid and Schubert, 1995). The amplitude of a Hough mode and the latitudinal shape of the Hough function determine the significance of any particular tidal variation at a specific latitude. The Hough functions for the migrating tides (same local time dependence at all longitudes, $\cos(\omega t_{LT} + s\lambda - \phi)$, where ϕ is independent of longitude (λ)) vanish at the Poles and their amplitudes at very high latitudes are very small. On the other hand, Hough functions for zonally symmetric tides ($s=0$) (same universal time dependence at all longitudes, $\cos(\omega t_{UT} - \phi)$, where ϕ is independent of longitude) can have maxima at the Poles. Hence, they dominate at very high latitudes (Longuet-Higgins, 1968). While, for migrating tides the phase varies with longitude by $s\lambda$, for zonally symmetric oscillations the phase is the same when observed simultaneously at different longitudes since $s=0$. Hence, except for longitude separation satisfying the condition $s\Delta\lambda = 2\pi n$, oscillations observed si-

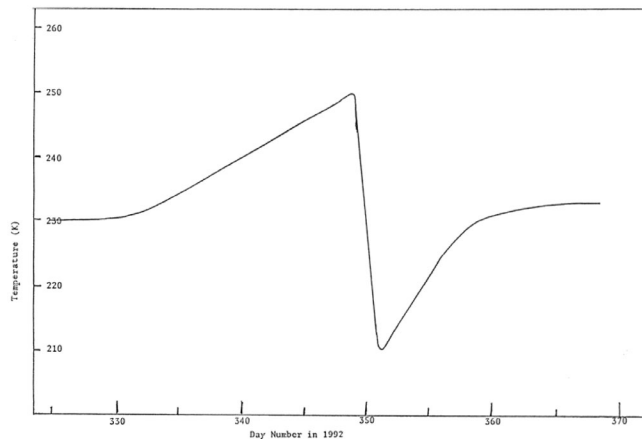


Fig. 2. Mesopause Temperature Variations During SWE

multaneously at about the same latitude but different longitudes will show phase difference of $s\Delta\lambda$ for migrating tides and zero phase for zonally symmetric tides. Figure 1, displays the phase spectrum of airglow OH emissions from two mesopause regions located at the same latitude but separated 120° in longitude. For migrating tides, the phase difference in the observations from these two regions should be 180° , yet all our measurements from the Polar region indicate, as exemplified in Figure 1, that the phase difference is very close to zero for all observed oscillation periods between 2 and 96 hours. Hence, the Polar MLT air density and temperature oscillations (with periods = 24 hours/ n , $n=1,2,3..$) are most likely the manifestation of the effects of zonally symmetric tides in the Polar region (Walterscheid and Sivjee, 2001).

Figure 2 shows that between 18th and 23rd, February, 1993, the Mesopause air temperature over Eureka ($80^\circ N$) dropped by about 30 K from its average value earlier that month (Walterscheid et al., 2001). Concurrent Lidar observations, at the same site where the airglow measurements were made, showed Stratospheric Warming Event (SWE) by the same amount (Whiteway and Carswell, 1994). However, the Mesopause cooling began earlier than the SWE, which implies that the Mesopause region was effectively below the reach of the heat fluxes forced by the stationary planetary waves during the SWE (Walterscheid et al., 2001). The latter occurred when the Polar Vortex core (which is warmer in the upper Stratosphere than in the region outside the core) moved over Eureka (Duck et al., 1998). It indicates the combined effects of the zonal mean transport associated with the SWE, variations due to Planetary waves and the motion of the vortex in which the Gravity wave activity may be enhanced (Duck et al., 1998). Numerical simulation in TIME-GCM model predicts the warming and cooling trend in the Stratosphere to Mesopause heights observed in the Lidar and the airglow OH emission spectral data (Walterscheid et al., 2001). However, the model underpredicts the extent of the observed Mesopause cooling. This may, in part, reflect the effects of Gravity waves. The latter may add to variations due to the SWE, which is caused by wave-mean flow interactions involving large-scale topographically forced stationary waves and critical levels (Matsuno, 1971).

Continuous long term Polar airglow observations show MLT air temperature and density modulations similar in period to Tropospheric and Stratospheric intraseasonal (IS) variations (Sivjee and Walterscheid, 2001). (The IS variations are observed in lower atmosphere data related to length-of-day, atmospheric angular momentum variations, outgoing long wave radiation and wind fields up to 10 hPa.) Fairly broadband spectral features centered around 17-, 23- and 45-days are evident in the spectrogram of MLT temperature and density variations derived from airglow emissions peaked in the MLT region. The 17-day oscillation of the Polar MLT region is more prominent in the lower atmosphere. This oscillation is most likely associated with the second symmetric $s = 1$ free Rossby mode. The Polar airglow data should not show this mode since the spectral components that produce such

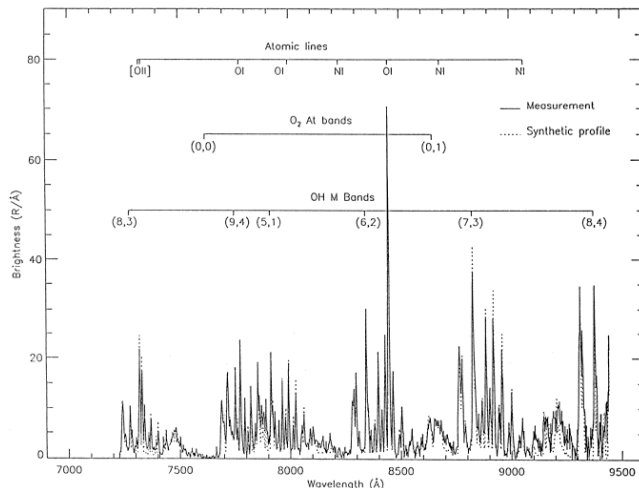


Fig. 3. Polar “Drizzle” Excited Optical Emissions Merged With Airglow

variations vanish in the Polar region. Also, free oscillations of zonal wave number zero with such long periods should not exist in the Polar MLT region. The observed 17-day oscillation is likely driven by the interaction between global Rossby mode and stationary wave number one Planetary waves.

3.2 Polar Cap Ionospheric Optical Emissions Excited by “PolarDrizzle”

Both satellite particle and ground-based optical observations point to an extensive region in the Polar Cap covered by precipitation of relatively low flux of soft electrons (Makita et al., 1991); (Newell and Meng, 1992). Not only does the Polar “drizzle” appear variable in temporal frequency and energy characteristics, but the spatial location and extent of the precipitating zone within the Polar Cap also changes with time. The DE (Craven et al., 1992) and VIKING (Murphree et al., 1992) satellite, as well as the Polar Bear satellite and ground-based optical observations, all show distinct zones of bright and dim particle-induced light in the Polar Cap, with the rest of the region inside the Auroral Oval devoid of such optical signatures of precipitating electrons. These observations are based on optical measurements that do not respond to extremely low light levels (\sim a few Rayleighs (R)) of particle-excited ionospheric emissions (Makita et al., 1991). Our CCD Spectrographs detect electron-excited OI 8446 Å emissions down to 0.1 R level. The Polar “drizzle” electrons dissipate most of their energy in the ionosphere where atomic species dominate. Thus the optical emissions from such events consist mostly of OI and OII lines. They are easily detected by our CCDS as shown in Figure 3.

3.3 Polar Auroral Arcs

Polar auroral arcs occur in the central Polar Cap during much of the time that the Inter Planetary Magnetic Field (IMF) B_z is positive. They also occur during major solar wind-magnetospheric shocks (following CMEs) (Steele et al., 1998) and occasionally as poleward expansions of the auroras dur-

ing substorms (McEwen, 1998). Morphological studies of these auroras (Zhang et al., 1999) suggest that polar auroras are potentially valuable indicators of the state of the magnetosphere and the solar wind. We have investigated the relation between our Polar measurements of OI 8446 Å emissions and the concurrent IMF and solar wind plasma data from the WIND satellite. In 84% of the 270 independent cases investigated, the Polar auroral OI 8446 Å emission was associated with positive (northward) IMF B_z . In the remaining 16% of the cases, the OI 8446 Å emission was observed in Polar Auroral arcs formed when the IMF B_z was negative. The relation between auroral OI 8446 Å brightness and the IMF B_z strength as well with solar wind dynamic pressure (P_{SW}) is nonlinear. These investigations also indicate that the larger the changes in B_z and the P_{SW} , the longer the time delay between the onset of changes in these solar parameters and the appearance of Polar Auroral arcs which excite the OI 8446 Å emission. Such observation suggest that when the magnetosphere is compressed during high B_z or P_{SW} conditions, there is a significant increase in the flux of auroral electrons precipitating in the central Polar Cap region (Zhang et al., 2001).

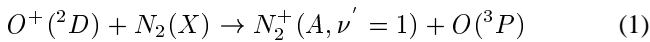
3.4 Polar F-Region Patches

Polar F-layer patches are characterized by enhanced [OI] 6300 Å emission from the ionosphere; the latter reflects changes in ionospheric electron density (n_e) and electron temperature (T_e). F-layer patches were first observed in the Polar Ionosphere, drifting across the Magnetic Pole, by (Weber et al., 1986). They are now recognized to occur much of the time that the IMF B_z is negative (McEwen and Harris, 1996). Rosenberg et al. (1993) observed a decrease in Polar “drizzle” in F-layer patches, and theoretical modeling of the patches, by Guzdar et al. (1998), predicts the presence of geomagnetic field aligned electric field associated with these patches. The latter would decelerate the Polar “drizzle” electrons and even reflect them back up the field lines. In this model, the F-layer patches should be devoid of significant level of electron excited emissions, such as OI 8446 Å line. Concurrent F-region patches and CCDS IR spectral observations indicate that [OI] 6300 Å enhancement in the F-layer patches are not due to precipitating electrons but most likely represent the effects of enhanced n_e and T_e .

3.5 Joule Heating

The effects of intense Joule heating events on the E-region kinetic temperature (T) is generally small. However, in the F-region, where the air density is at least an order of magnitude lower, changes in T may be significant. Polar auroral [OI] 6300 Å Doppler profiles show large T enhancements. Whether these measurements reflect changes in local T, or of distant regions from which the long-lived red emissions may have been excited and then convected to the observing sites, is unclear. Unfortunately, auroras which peak in the F-region are devoid of significant molecular band emissions that do

not involve resonant scattering of sunlight (Sivjee, 1983). An exception is the N_2^+ Meinel (1,0) band which results from the following resonant-energy charge exchange process:



followed by emission of Meinel (1,0) band. The spectral distribution of the latter yields T of the region where the above reaction occurs which is the same region from which the band emission originates.

Acknowledgements. This work was supported by the National Science Foundation through grants # ATM-9804674, OPP-9909339 and OPP-9910950 as well as by the National Aeronautics and Space Administration through grant # NAG5-10066-0001.

References

- Craven, J. D., L. A. Frank, J. S. Murphree, L. L. Cogger, J. D. Winingham and R. A. Heelis, Auroral observations in the two polar caps, *EOS Trans.*, AGU, 73 (14), Spring meeting suppl., 221, 1992.
- Duck, T. J., J. A. Whiteway and A. I. Carswell, Lidar observations of gravity wave activity and Arctic stratospheric vortex core warming, *Geophys. Res. Lett.*, 25, 2813, 1998.
- Guzdar, P. N., et al., 3D nonlinear simulations of the gradient drift instability in the high latitude ionosphere, *Rad. Science*, 33, 1901-1913, 1998.
- Longuet-Higgins, M. S., The eigen functions of Laplace's tidal equations over a sphere, *Philosophical Transactions of The Royal Society*, London, Ser. A, 262, 511, 1968.
- Makita, K., C. I. Meng and S. I. Akasofu, Transpolar auroras, their particle precipitation, and IMF B_z component, *J. Geophys. Res.*, 96, 14085, 1991.
- Matsuno, T., A dynamical model of the stratospheric sudden warming, *J. Atmos. Sci.*, 28, 1479, 1971.
- McEwen, D. J., Electron precipitation observations from a rocket flight through the dayside auroral oval, *Planet. Space Sci.*, 25, 1161, 1977.
- McEwen, D. J., and D. A. Harrington, Polar airglow and aurora, *Canadian J. Phys.*, 69, 1055, 1991.
- McEwen, D. J. and D. P. Harris, Occurrence patterns of F layer patches over the north magnetic pole, *Radio Sci.*, 31, 619-628, 1996.
- McEwen, D. J., Ionospheric dynamics in the central polar cap, *Advances in Space Res.*, 17, in press, 1998.
- Murphree, J. S., L. L. Cogger and R. D. Elphinstone, High latitude auroral phenomena observed by the Viking UV imager, *EOS Trans. AGU*, 73 (14), Spring meeting suppl., 221, 1992.
- Newell, P. T. and C. I. Meng, Mapping the dayside ionosphere to the magnetosphere according to the particle precipitation characteristics, *Geophys. Research Letters*, 19, 609, 1992.
- Rosenberg, T., et al., Imaging riometer and HF radar measurements of drifting electron density structures in the polar cap, *J. Geophys. Res.*, 98, 7757, 1993.
- Sivjee, G. G., Difference in near UV (~ 3400 - 4300\AA) optical emissions from mid-day cusp and nighttime auroras, *J. Geophys. Res.*, 88, 435, 1983.
- Sivjee, G. G., R. L. Walterscheid and D.J. McEwen, Planetary wave disturbances in the arctic winter mesopause over Eureka (80° N), *Planet-Space Sci.*, 42, 973, 1994.
- Sivjee, G. G. and D. Shen, Auroral optical emissions during the solar magnetic cloud event of October 1995, *J. Geophys. Res.*, 102, 7431, 1997.
- Sivjee, G. G. and R. L. Walterscheid, Low-frequency intra-seasonal variations of the wintertime very high latitude mesopause regions, *submitted to J. Geophys. Res.*, 2001.
- Steele, D. P., D. J. McEwen and G. G. Sivjee, Ground-based optical observations from the north magnetic pole during the January 1997 magnetic cloud event, *Geophys. Res. Lett.*, 25, 2573, 1998.
- Thayer, J., Height-resolved joule heating rates in the high latitude E region and the influence of neutral winds, *J. Geophys. Res.*, 103, 471, 1998.
- Walterscheid, R. L. and G. Schubert, A dynamical chemical model of fluctuations in the OH airglow driven by migrating tides, stationary tides and planetary waves, *J. Geophys. Res.*, 100, 17,433, 1995.
- Walterscheid, R. and G. G. Sivjee, Zonally symmetric oscillations observed in the airglow from South Pole station, *J. Geophys. Res.*, 106, 3645, 2001.
- Walterscheid, R. L., G. G. Sivjee and R. G. Roble, Mesospheric and lower thermospheric manifestations of a stratospheric warming event over Eureka, Canada (80° N), *Geophys. Res. Lett.*, 2001.
- Weber, E. J., J. A. Klobuchar, J. Buchau, H. C. Carlson et al, Polar cap F patches: Structures and dynamics, *J. Geophys. Res.*, 91, 121-129, 1986.
- Whiteway, J. A. and A. I. Carswell, Rayleigh lidar observations of thermal structure and gravity wave activity in the High Arctic during a stratospheric warming, *J. Atmos. Sci.*, 51, 3122, 1994.
- Zhang, Y., D. J. McEwen and I. Oznovich, Solar wind density enhancements and central polar arcs, *Advance in Space Research*, 22, 1305, 1998.
- Zhang, Y., D. J. McEwen and W. Guo, Polar ionospheric response to solar wind IMF changes, *J. Geophys. Research*, 1999.
- Zhang, Y., D. J. McEwen and G. G. Sivjee, IMF B_z control of polar auroral infrared emissions, *submitted to J. Geophys. Research*, 2001.